JACS
JOURNAL OF THE AMERICAN CHEMICAL SOCIETY
Communication
pubs.acs.org/JACS

Poly(ethylene oxide) Functionalized Graphene Nanoribbons with Excellent Solution Processability

Yinjuan Huang,[†] Yiyong Mai,[*,†] Uliana Beser,[‡] Joan Teyssandier,[§] Gangamallaiah Velpula,[§] Hans van Gorp,[§] Lasse Arnt Straasø,[∥] Michael Ryan Hansen,[⊥] Daniele Rizzo,[#] Cinzia Casiraghi,[#] Rong Yang,[▽] Guangyu Zhang,[▽] Dongqing Wu,[†] Fan Zhang,[†] Deyue Yan,[†] Steven De Feyter,[§] Klaus Müllen,[‡] and Xinliang Feng[*,†,◆]

[†]School of Chemistry and Chemical Engineering, Shanghai Jiao Tong University, 800 Dongchuan RD, Shanghai 200240, China
[‡]Max Planck Institute for Polymer Research, Ackermannweg 10, 55128 Mainz, Germany
[§]Division of Molecular Imaging and Photonics, Department of Chemistry, KU Leuven Celestijnenlaan, 200 F, B-3001 Leuven, Belgium
[∥]Interdisciplinary Nanoscience Center, Aarhus University, Gustav Wieds Vej 14, DK-8000 Aarhus C, Denmark
[⊥]Institute of Physical Chemistry, Westfälische Wilhelms-Universität Münster, Corrensstr. 28/30, D-48149 Münster, Germany
[#]School of Chemistry, Manchester University, Oxford Road, Manchester M139PL, United Kingdom
[▽]Institute of Physics, Chinese Academy of Sciences, P.O. Box 603, Beijing 100190, China
[◆]Department of Chemistry and Food Chemistry, Technische Universität Dresden, Mommsenstrasse 4, 01062 Dresden, Germany

Supporting Information

ABSTRACT: Structurally well-defined graphene nanoribbons (GNRs) have attracted great interest as next-generation semiconductor materials. The functionalization of GNRs with polymeric side chains, which can widely broaden GNR-related studies on physiochemical properties and potential applications, has remained unexplored. Here, we demonstrate the bottom-up solution synthesis of defect-free GNRs grafted with flexible poly(ethylene oxide) (PEO) chains. The GNR backbones possess an armchair edge structure with a width of 1.0−1.7 nm and mean lengths of 15−60 nm, enabling near-infrared absorption and a low bandgap of 1.3 eV. Remarkably, the PEO grafting renders the GNRs superb dispersibility in common organic solvents, with a record concentration of ∼1 mg mL^{-1} (for GNR backbone) that is much higher than that (<0.01 mg mL^{-1}) of reported GNRs. Moreover, the PEO-functionalized GNRs can be readily dispersed in water, accompanying with supramolecular helical nanowire formation. Scanning probe microscopy reveals raft-like self-assembled monolayers of uniform GNRs on graphite substrates. Thin-film-based field-effect transistors (FETs) of the GNRs exhibit a high carrier mobility of ∼0.3 cm^2 V^{-1} s^{-1}, manifesting promising application of the polymer-functionalized GNRs in electronic devices.

Graphene nanoribbons (GNRs) have attracted great attention as candidates for next-generation semiconductor materials.[1−3] Their electronic properties, such as the finite bandgap, are strongly governed by their width and edge structures. Among a number of "top-down"[1,4,5] and "bottom-up"[2,6−10] approaches developed for the fabrication of GNRs, bottom-up solution synthesis shows an incomparable advantage in large-scale production of liquid-phase-processable GNRs with well-defined structures.[2,6,7] Nevertheless, chemically synthesized GNRs either have no side substituents or are functionalized only with short alkyl chains,[2,7,11,12] which greatly limits their solution processability and thus impedes their deeper fundamental studies and prospective applications. Attachment of polymer chains to GNR backbones would offer a promising strategy to surmount this barrier. This approach, however, has remained unexplored.

Here, we demonstrate the bottom-up solution synthesis of GNRs grafted with flexible poly(ethylene oxide) (PEO) chains, which involves the pre-introduction of methoxycarbonyl and carboxylic active groups on the periphery of GNRs (Scheme 1). The PEO-functionalized GNRs (GNR-PEO) have a PEO grafting percentage (GP) of 46% and shows excellent dispersibility in common organic solvents such as tetrahydrofuran (THF), with high concentrations of up to ∼1 mg mL^{-1} (for the GNR backbone), superior to those of reported GNRs (<0.01

Scheme 1. Synthetic Route Towards PEO-Functionalized GNRs

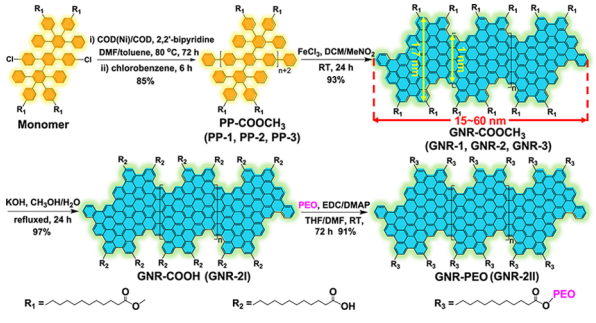

Received: July 8, 2016
Published: July 27, 2016

DOI: 10.1021/jacs.6b07061
J. Am. Chem. Soc. 2016, 138, 10136−10139

mg mL^{-1}).[2,3] UV−vis studies of GNR-PEO in THF revealed a near-infrared (NIR) absorption with the maximum at ~650 nm and an optical bandgap of ~1.3 eV. Interestingly, GNR-PEO was water-dispersible, exhibiting red-shifted absorption bands, which are associated with the formation of helical nanowire superstructure of the GNRs. Photoluminescence (PL) spectrometry unveiled NIR emission with the maximum at ~920 nm for GNR-PEO in THF, while complete PL quenching was detected for the GNRs in aqueous solution. Scanning probe microscopy (SPM) analysis of GNR-PEO deposited on graphite substrates revealed a raft-like ordered self-assembled monolayer structure. The excellent solution processability of GNR-PEO allowed the fabrication of thin-film-based field-effect transistors (FETs) by directly drop-casting their THF dispersions on Si/SiO_2 substrates, exhibiting a high carrier mobility of ~0.3 $cm^2\ V^{-1}\ s^{-1}$, which is superior to those of GNR thin-film based FETs reported previously.[13,14]

The chemical synthesis toward GNR-PEO is illustrated in Scheme 1, and the detailed procedures are described in the Supporting Information (SI). First, laterally expanded poly-*para*-phenylene decorated with $-C_{10}H_{20}COOCH_3$ chains (named as PP-$COOCH_3$) was prepared by AA-type Yamamoto polymerization of a dichloro-substituted oligophenylene monomer.[15] The successful synthesis of PP-$COOCH_3$ was demonstrated by nuclear magnetic resonance (NMR) and gel permeation chromatography (GPC) studies (Figures S1−S3).[15] GPC analyses against polystyrene standard revealed that the PP-$COOCH_3$ samples had different number-average molecular weights (M_ns) ranging from 20,000 to 80,000 as well as narrow polydispersity indices (PDI) of 1.06−1.12 (PP-1, PP-2, and PP-3 in Table 1). Second, the PP-$COOCH_3$ samples were transformed into GNRs with a *para*-armchair edge structure as well as a width of 1.0−1.7 nm and different calculated average lengths of 15−60 nm (Scheme 1 and Table 1), by employing intramolecular cyclodehydrogenation in CH_2Cl_2 solution using $FeCl_3$ as the Lewis acid and oxidant.[7] As PP-2 with the M_n of ~40,000 was easier to obtain by the Yamamoto polymerization in the present study, the synthesis of GNR-2 with a mean length of ~30 nm could be readily scaled up to the gram scale. Third, the hydrolysis of GNR-2 yielded GNR-COOH, where the carboxyl groups afforded opportunities for further modification of the GNRs. Finally, GNR-PEO with a PEO grafting percentage of 46% was achieved by the esterification of the carboxyl groups in GNR-COOH with the hydroxyl groups at one end of 1 kg/mol PEO chains (Scheme 1).

Table 1. GPC Data of PP-$COOCH_3$ Samples and Lengths of the Corresponding GNRs

PP-$COOCH_3$	M_n (g/mol)	PDI	GNR-$COOCH_3$	GNR-COOH	GNR-PEO	GNR length (nm)[a]
PP-1	19,900	1.06	GNR-1	–	–	~15
PP-2	42,300	1.12	GNR-2	GNR-2I	GNR-2II	~30
PP-3	82,100	1.10	GNR-3	–	–	~60

[a]The lengths are calculated based on M_n of the polyphenylene precursors

Fourier transform infrared (FTIR) analyses reveal significant attenuation of the signals from aromatic C−H stretching vibrations at 3083, 3050, and 3024 cm^{-1} as well as the out-of-plane (*opla*) C−H deformation bands at 829, 809, and 698 cm^{-1} in the spectrum of GNR-$COOCH_3$ compared with that of PP-$COOCH_3$ (Figures S10−12).[7,16,17] In addition, typical *opla* bands for aromatic C−H at the armchair edge of the GNR basal plane appear at 816 and 861 cm^{-1}.[7,18] These results validate the efficient "graphitization" of the polyphenylene backbone into GNR.[2,7] The FTIR spectrum of GNR-PEO (Figure S14) shows a distinct increase in intensity of the band at 1730 cm^{-1} (the stretching of C═O in ester group) and an attenuation of the signal at 1702 cm^{-1} (the stretching of C═O in carboxyl group), demonstrating the successful grafting of the PEO chains. The ^{13}C solid-state NMR analysis reveals a grafting percentage of 46% for GNR-PEO, which is supported by the calculation based on thermogravimetric analysis (Figures S15−16 and pp S18−19, SI). Moreover, solid-state ^1H NMR spectroscopy reveals that PP-$COOCH_3$, with a semiflexible to semirigid structure, becomes rigid and planar after graphitization into GNR (Figure S17).[2,3] Specifically, the 2D $^1H-^1H$ double quantum−single quantum (DQ-SQ) correlation spectra show broad, stretched, and split ridge signals in the aromatic regions (Figure S17), which originate from the interactions between the two types of aromatic protons at the edge of the GNRs, confirming the graphitization of PP-$COOCH_3$.[2,3]

The Raman spectra of the resulting GNRs exhibit typical D and G peaks (Figures 1a and S18), as reported for other GNRs.[2,7,19] Figure 1a shows that the first-order Raman spectrum is not strongly dependent on the functionalization of the GNRs. Importantly, a distinct peak, associated with the radial breathing-like mode (RBLM),[2,8] is observed at ~170 cm^{-1} for all GNR samples. The presence of this peak confirms the atomically precise and low-dimensional structure of GNRs.[2,19] By using the relation: $w = 3222/\nu_{RBLM}$ Å, where w is the width and ν_{RBLM} is the RBLM wavenumber,[2,3] the mean width of our GNRs is experimentally estimated to be ~1.9 nm, which is in good agreement with the calculated value of 1.7 nm (Scheme 1). The RBLM of these GNRs seems to be less affected by the edge pattern geometry, compared to other GNRs, where a strong discrepancy between experimental and calculated RLBM position has been observed.[19]

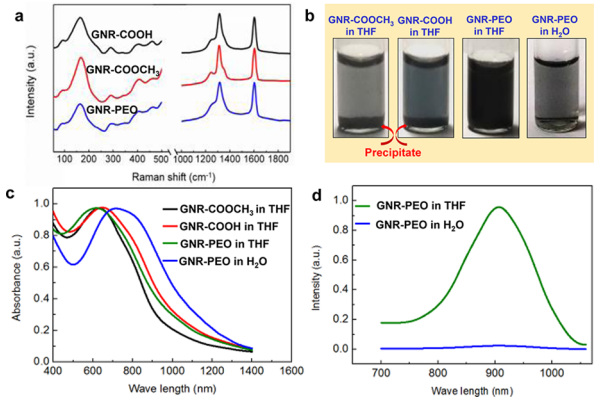

Figure 1. (a) Raman spectra of the GNRs with identical mean lengths of ~30 nm (excited at 638 nm). (b) Photos of GNR dispersions in THF (1.0 mg mL^{-1} for GNR backbone) and in H_2O (0.2 mg mL^{-1}) after sonication for 5 min. (c) UV−vis spectra of GNR dispersions (0.01 mg mL^{-1}). (d) PL spectra of CNR-PEO dispersions (0.01 mg mL^{-1}).

Owing to the high-degree grafting of PEO chains, the resultant GNRs exhibit superior dispersibility in conventional organic solvents including THF, chloroform, chlorobenzene, and 1,2,4-trichlorobenzene (TCB), etc. Mild sonication of GNR-PEO in these organic solvents, e.g., in THF, generated black homoge-

DOI: 10.1021/jacs.6b07061
J. Am. Chem. Soc. 2016, 138, 10136−10139

neous dispersions with high concentrations up to ~1 mg mL^{-1} (for GNR backbone, Figure 1b). The dispersions were stable without visual precipitation for at least 1 day. In sharp contrast, GNR-$COOCH_3$ and GNR-COOH could not be homogeneously dispersed in these solvents under similar experimental conditions, and a visible precipitate was observed within several minutes after sonication (Figure 1b). The highest concentrations of GNR-$COOCH_3$ and GNR-COOH in THF only reached ~0.02 and ~0.05 mg mL^{-1}, respectively (Figure S20). Moreover, the dispersibility of GNR-PEO is much better than that of reported alkylated GNRs (<0.01 mg mL^{-1} in dispersions).[2,3] On the other hand, dynamic light scattering (DLS) analysis gave a single narrow size distribution with an average hydrodynamic diameter (D_h) of ~40 nm for GNR-PEO in THF (Figure S21). The fact that the mean D_h is close to the calculated size (~30 nm) of a single PEO-modified GNR suggests the lack of serious aggregation of GNR-PEO in THF. This result contrasts starkly to those from reported alkylated GNRs, which suffer from pronounced aggregation under similar conditions.[2,3]

Remarkably, GNR-PEO was also water-dispersible with a high concentration of ~0.2 mg mL^{-1} of the GNR backbone (Figure 1b). The dispersions were stable for several hours depending on the concentration. DLS study gave a much increased mean D_h (~450 nm) for GNR-PEO in H_2O, suggesting supramolecular assembly of the GNRs (Figure S21). Transmission electron microscopy and AFM revealed an interesting helical nanowire superstructure for the GNR assemblies, which has a mean diameter of 25 ± 12 nm, lengths of 5−20 μm and an average pitch of 48 nm (Figure S22).

The excellent dispersibility of GNR-PEO in common solvents offers opportunities for a wide range of solution-based physical characterizations. UV−vis spectrum of GNR-PEO in a dilute THF dispersion reveals NIR absorption with the maximum at ~650 nm and an optical bandgap of ~1.3 eV (Figure 1c). This bandgap agrees well with the calculated value of 1.34 eV for *para*-armchair edge GNRs based on density functional theory.[20] The absorption spectra of GNR-$COOCH_3$ and GNR-COOH in THF display similar features to that of GNR-PEO (Figure 1c). In contrast, GNR-PEO in H_2O exhibits a significantly red-shifted main absorption band associated with a lower bandgap of ~1.0 eV (Figure 1d). On the other hand, the GNRs with different mean lengths of 15−60 nm exhibit an identical bandgap of 1.3 eV (Figure S23), suggesting negligible longitudinal confinement in determining the bandgaps of GNRs of over 15 nm in length. As serious aggregation generally quenches the fluorescence of GNRs, their PL characteristics have been difficult to obtain. In our work, GNR-PEO in dilute THF dispersion gave a PL spectrum with the emission maximum at ~920 nm (Figure 1d), attributable to the outstanding dispersibility of GNR-PEO. In contrast, GNR-PEO in H_2O shows complete PL quenching due to the strong aggregation of the GNRs.

Self-assembled monolayers of GNR-PEO were investigated at the liquid−solid interface by means of scanning tunnel microscopy (STM). Figure 2a displays a typical STM image of GNR-PEO deposited on highly oriented pyrolytic graphite (HOPG) using hot TCB, which reveals small domains of self-assembled GNRs where individual GNRs are coaligned side by side into a lamellar structure. The average longitudinal size (>100 nm) of the lamellae is larger than the length of a single GNR, indicating an end-to-end alignment of the GNRs within a lamella. The periodicity of these stripes is in the range of 5.1−5.7 nm, much lower than the width of a GNR-PEO with fully extended side-chains. This suggests that the PEO chains either form

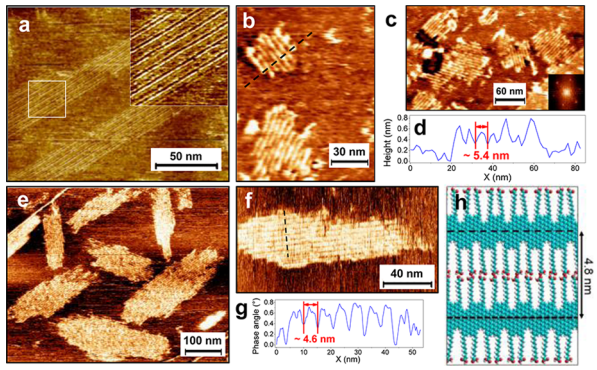

Figure 2. (a) STM image of isolated GNR-PEO domains at the TCB/HOPG interface (I_{set} = 100 *p*A, V_{bias} = −0.6 V). (b, c) AFM topography images of self-assembled GNR-PEO monolayers on HOPG upon drying. Inset in (c) shows a Fourier transform of the image showing the three axes of the 5.4 nm wide lamellas. (d) Line profile along the black dotted line in the AFM image in panel (b) shows the formation of a monolayer film. (e, f) AFM phase images of isolated GNR-COOH domains on HOPG upon drying. (g) Line profile along the black dotted line in panel (f) shows a periodicity of 4.6 nm for the lamellae. (h) A molecular model depicting the plausible arrangement of GNR-COOH in the organized monolayers. In this model, alkyl chains are fully extended and adjacent molecules possibly interact with each other via hydrogen bonding of the terminal carboxyl groups; the GNRs parallel to each other without stacking or interdigitation of the alkyl chains. The periodicity is 4.8 nm.

coiled/entangled bundles between the aromatic backbones of adjacent GNRs or are back-folded in the supernatant solution. Similar behavior was reported earlier where oligoethylene oxide chains remain in solution due to their lower adsorption energy on graphite compared with alkyl chains.[21] Besides, the lamellae appear as a repetition of double bright stripes sandwiching a dark one, which could be induced by the introduction of the PEO chains. Lamellae of various sizes (tens of nm) on HOPG were also imaged by atomic force microscopy (AFM) after evaporation of the solvent (Figure S25), including assemblies of only a few GNRs and even stripes compatible with single GNRs (Figure 2b,c). A line profile traced on the AFM image shows a height difference of ~0.4 nm between graphite and the GNRs (Figure 2d), validating the formation of organized monolayers. The average periodicity of the stripes in the lamellae is 5.4 ± 0.3 nm, in agreement with the result from STM.

In comparison, AFM analysis of GNR-COOH dry films on HOPG revealed similar monolayer structures with striped domains (Figure 2e,f). The mean periodicity of the stripes in a GNR-COOH lamella is 4.6 ± 0.2 nm (Figure 2g), which is in accordance with the calculated assembly model of GNR-COOH (periodicity: 4.8 nm, Figure 2h). The 0.8 ± 0.5 nm difference in periodicity between the two types of GNRs can be explained by the insertion of PEO "rows" in the lamellae, the interactions of which allows the organization of GNR-PEO into a regular pattern.

Profiting from the excellent dispersibility of GNR-PEO in common organic solvents, we investigated the electronic properties of the GNRs by fabricating GNR-based thin-film FETs. To this end, GNR-PEO was deposited between Ti/Au electrodes on Si/SiO_2 substrate by drop-casting of the dispersion (0.5 mg mL^{-1}) in THF (Figure S27A). The subsequent mild heating vaporized THF rapidly and left a GNR thin film behind without solvent contamination, which is a great advantage of low-boiling solvents. Afterward, the substrate was annealed under a

DOI: 10.1021/jacs.6b07061
J. Am. Chem. Soc. 2016, 138, 10136−10139

H_2/Ar atmosphere at 500 °C, which is an optimum temperature to cut off the insulating alkyl chains from GNRs to reduce ribbon-to-ribbon junction resistance without affecting the GNR basal plane.[13] FTIR and Raman spectroscopies of the film revealed no apparent influence of the thermal treatment on the GNR backbone (Figure S28A,B). Moreover, the GNR thin film between two Ti/Au electrodes was imaged by SEM and AFM, which gave a length of ~3 μm, a width of ~3 μm, and a thickness of ~27 nm for the film (Figures S27B and S28C). In contrast, GNR-$COOCH_3$ and GNR-COOH could only form discontinuous films with massive aggregates on the substrate under the similar drop-casting conditions, attributable to their much poorer dispersibility in THF.

The current vs drain voltage ($I-V_d$) and current vs gate voltage ($I-V_{gs}$) for the channel length $L \sim 3$ μm thin-film FET are displayed in Figure S27C,D. The $I-V_d$ curves of the thin film before and after annealing at 500 °C prove that annealing can significantly increase the conduction (inset in Figure S27C). The thin-film FET exhibited maximum carrier mobility of ~0.3 cm^2 V^{-1} s^{-1} and an on−off ratio of ~4 under a low voltage of 20 V (Figure S27D, the calculation is provided in the SI, p S29). Although the GNR thin film still revealed a limited p-type current modulation, which is probably due to the electric-field screening effect in GNR films and relatively high ribbon-to-ribbon junction resistance,[22,23] the resultant mobility represents the best among those of GNR-thin-film based FETs reported thus far.[13,14]

In summary, we demonstrated the first bottom-up solution synthesis of polymer-functionalized GNRs with defined structures. The resultant GNR-PEO exhibited an outstanding dispersibility in common organic solvents and even water. The excellent dispersibility offers opportunities not only for deep understanding physiochemical properties of GNRs by a wide range of solution-based physical characterizations including UV−vis, PL, DLS, and SPM, etc., but also for developing prospective applications such as GNR-thin-film based FETs. This study blazes a trail for polymer functionalization of GNRs, which holds promise to prepare thin films with controlled alignment of GNRs by solution deposition. This means might enhance the electrical properties of bottom-up synthesized GNRs. Moreover, polymer functionalization affords chances to develop new GNR-related studies in a broad range of research areas including molecular self-assembly, nanocomposites, and biotechnology, etc.

■ ASSOCIATED CONTENT

Supporting Information

The Supporting Information is available free of charge on the ACS Publications website at DOI: 10.1021/jacs.6b07061.

Experiment details and data (PDF)

■ AUTHOR INFORMATION

Corresponding Authors

*mai@sjtu.edu.cn

*xinliang.feng@tu-dresden.de

Notes

The authors declare no competing financial interest.

■ ACKNOWLEDGMENTS

This work was financially supported by the 973 Programs of China (2013CBA01602), the Natural Science Foundation of China (21320102006, 21304057, and 51573091), the MPI Partner Group Project for Polymer Chemistry of GNRs, EC under Graphene Flagship (no. CNECT-ICT-604391), the European Union's Seventh Framework Programme (FP7/2007-2013)/ERC grant (no. 340324), and the Villum Foundation under the Young Investigator Programme (VKR023122). The authors also thank the Center for Advancing Electronics Dresden (CFAED) and the Instrumental Analysis Center of Shanghai Jiao Tong University for some measurements.

■ REFERENCES

(1) Wang, X.; Dai, H. *Nat. Chem.* **2010**, *2*, 661.

(2) Narita, A.; Feng, X.; Hernandez, Y.; Jensen, S. A.; Bonn, M.; Yang, H.; Verzhbitskiy, I. A.; Casiraghi, C.; Hansen, M. R.; Koch, A. H. R.; Fytas, G.; Ivasenko, O.; Li, B.; Mali, K. S.; Balandina, T.; Mahesh, S.; De Feyter, S.; Müllen, K. *Nat. Chem.* **2013**, *6*, 126.

(3) Narita, A.; Verzhbitskiy, I. A.; Frederickx, W.; Mali, K. S.; Jensen, S. A.; Hansen, M. R.; Bonn, M.; De Feyter, S.; Casiraghi, C.; Feng, X.; Müllen, K. *ACS Nano* **2014**, *8*, 11622.

(4) Li, X.; Wang, X.; Zhang, L.; Dai, H. *Science* **2008**, *319*, 1229.

(5) Kosynkin, D. V.; Higginbotham, A. L.; Sinitskii, A.; Lomeda, J. R.; Dimiev, A.; Price, B. K.; Tour, J. M. *Nature* **2009**, *458*, 872.

(6) Yang, X.; Dou, X.; Rouhanipour, A.; Zhi, L.; Müllen, K. *J. Am. Chem. Soc.* **2008**, *130*, 4216.

(7) Schwab, M.; Narita, A.; Hernandez, Y.; Balandina, T.; Mali, K. S.; De Feyter, S.; Feng, X.; Müllen, K. *J. Am. Chem. Soc.* **2012**, *134*, 18169.

(8) Cai, J.; Ruffieux, P.; Jaafar, R.; Bieri, M.; Braun, T.; Blankenburg, S.; Muoth, M.; Seitsonen, A. P.; Saleh, M.; Feng, X.; Müllen, K.; Fasel, R. *Nature* **2010**, *466*, 470.

(9) Cai, J.; Pignedoli, C. A.; Feng, X.; Müllen, K.; Fasel, R. *Nat. Nanotechnol.* **2014**, *9*, 896.

(10) Ruffieux, P.; Wang, S.; Yang, B.; Sánchez-Sánchez, C.; Liu, J.; Dienel, T.; Talirz, L.; Shinde, P.; Pignedoli, C. A.; Passerone, D.; Dumslaff, T.; Feng, X.; Müllen, K.; Fasel, R. *Nature* **2016**, *531*, 489.

(11) Vo, T. H.; Shekhirev, M.; Kunkel, D. A.; Morton, M. D.; Berglund, E.; Kong, L.; Wilson, P. M.; Dowben, P. A.; Enders, A.; Sinitskii, A. *Nat. Commun.* **2014**, *5*, 3189.

(12) Vo, T. H.; Shekhirev, M.; Kunkel, D. A.; Orange, F.; Guinel, M. J.-F.; Enders, A.; Sinitskii, A. *Chem. Commun.* **2014**, *50*, 4172.

(13) Abbas, A. N.; Liu, G.; Narita, A.; Orosco, M.; Feng, X.; Müllen, K.; Zhou, C. *J. Am. Chem. Soc.* **2014**, *136*, 7555.

(14) Gao, J.; Uribe-Romo, F. J.; Saathoff, J. D.; Arslan, H.; Crick, C. R.; Hein, S. J.; Itin, B.; Clancy, P.; Dichtel, W. R.; Loo, Y. L. *ACS Nano* **2016**, *10*, 4847.

(15) Huang, Y.; Mai, Y.; Yang, X.; Beser, U.; Liu, J.; Zhang, F.; Yan, D.; Müllen, K.; Feng, X. *J. Am. Chem. Soc.* **2015**, *137*, 11602.

(16) Centrone, A.; Brambilla, L.; Renouard, T.; Gherghel, L.; Mathis, C.; Müllen, K.; Zerbi, G. *Carbon* **2005**, *43*, 1593.

(17) Shifrina, Z. B.; Averina, M. S.; Rusanov, A. L.; Wagner, M.; Müllen, K. *Macromolecules* **2000**, *33*, 3525.

(18) Wu, J. S.; Gherghel, J.; Watson, M. D.; Li, J.; Wang, Z.; Simpson, C. D.; Kolb, U.; Müllen, K. *Macromolecules* **2003**, *36*, 7082.

(19) Verzhbitskiy, I. A.; Corato, M. D.; Ruini, A.; Molinari, E.; Narita, A.; Schwab, M. G.; Bruna, M.; Yoon, D.; Milana, S.; Feng, X.; Müllen, K.; Ferrari, A. C.; Casiraghi, C.; Prezzi, D. *Nano Lett.* **2016**, *16*, 3442.

(20) Osella, S.; Narita, A.; Schwab, M. G.; Hernandez, Y.; Feng, X.; Müllen, K.; Beljonne, D. *ACS Nano* **2012**, *6*, 5539.

(21) Chen, L.; Mali, K. S.; Puniredd, S. R.; Baumgarten, M.; Parvez, K.; Pisula, W.; De Feyter, S.; Müllen, K. *J. Am. Chem. Soc.* **2013**, *135*, 13531.

(22) Do, J. W.; Estrada, D.; Xie, X.; Chang, N. N.; Mallek, J.; Girolami, G. S.; Rogers, J. A.; Pop, E.; Lyding, J. W. *Nano Lett.* **2013**, *13*, 5844.

(23) Sangwan, V. K.; Ortiz, R. P.; Alaboson, J. M.; Emery, J. D.; Bedzyk, M. J.; Lauhon, L. J.; Marks, T. J.; Hersam, M. C. *ACS Nano* **2012**, *6*, 7480.

DOI: 10.1021/jacs.6b07061
J. Am. Chem. Soc. 2016, 138, 10136−10139